Uniform distribution of *35S* promoter-driven mDII auxin control sensor in leaf primordia

*Chunmei Guan[1], Fei Du[1], and Yuling Jiao[1,2]**

[1]State Key Laboratory of Plant Genomics, Institute of Genetics and Developmental Biology, Chinese Academy of Sciences, and National Center for Plant Gene Research, Beijing 100101, China

[2]College of Life Sciences, University of Chinese Academy of Sciences, Beijing 100049, China

*Author for correspondence: Yuling Jiao (yljiao@genetics.ac.cn)

Keywords: 35S, auxin, DII, leaf

Abstract

The DII sensor has been an invaluable tool to map spatiotemporal auxin response and distribution in the model plant *Arabidopsis thaliana.* The DII sensor and mDII control sensor are driven by the widely used constitutive *35S* promoter. However, the reliability of DII sensor has recently been questioned (Bhatia and Heisler, 2018). Here we provide additional evidence to show that the mDII control sensor is indeed uniformly distributed in early leaf primordia, which echoes the original reports (Vernoux et al., 2011; Brunoud et al., 2012). We also provide comparison between DII/mDII and the *PRS5A* promoter-driven R2D2 sensors in early leaf primordia.

Main text

Auxin is a classical phytohormone that serves as a plant morphogenetic signal throughout the life cycle. Spatiotemporal distribution of auxin response is pivotal to understanding auxin's role in pattern formation. DII-Venus is a recently developed auxin sensor, in which the fast maturing Venus fluorescent protein is fused in-frame to the auxin dependent degradation domain II of an Aux/IAA protein (Vernoux et al., 2011; Brunoud et al., 2012). It has been shown that the abundance of DII-Venus is dependent

on auxin, the TIR1/AFBs co-receptors, and proteasome activities. In the original design, DII-Venus is driven by the widely used constitutive *35S* promoter. The control sensor, mDII-Venus, has a mutation in the domain II sequence of DII-Venus, thus lacking auxin-dependent degradation. The mDII-Venus control sensor is also driven by the constitutive *35S* promoter. Comparing with mDII-Venus, stronger DII-Venus signal would indicate lower auxin. The DII-Venus sensor allows sensitive detection of auxin signaling at the cellular resolution in different tissues, and has been widely used, including in the field of plant development. An alternative design, named R2D2, combines DII-Venus and mDII-tdTomato into a single transgene (Liao et al., 2015). In addition, the R2D2 uses the *RPS5A* promoter instead of the *35S* promoter.

The *35S*-driven mDII-Venus has uniform expression in the vegetative shoot apex, including the shoot apical meristem (SAM) and young leaf primordia (Fig. 2h in Brunoud et al., 2012; Supplementary Fig. 7b in Vernoux et al., 2011), making it possible to use the *35S*-driven DII-Venus to map auxin signaling. Compared with mDII-Venus, DII-Venus shows clearly stronger signal in the adaxial domain facing the SAM in the first two leaves five days after stratification (DAS) (Fig. 2f,h in Brunoud et al., 2012; Supplementary Fig. 7a in Vernoux et al., 2011). We observed similar patterns in early leaf primordia of older plants (Qi et al., 2014; Guan et al., 2017), suggesting a transient abaxial-enrichment of auxin. These observations and the middle domain-enriched DR5 expression, together with genetics and molecular analysis, lead to a model, in which abaxial-enriched auxin, the adaxial-expressed auxin activator MONOPTEROS/AUXIN RESPONSE FACTOR5 (MP/ARF5), and abaxial-expressed ARF repressors together position auxin signaling in the middle domain (Guan et al., 2017). Auxin signaling activates *WUSCHEL-RELATED HOMEOBOX* (*WOX*) genes in the middle domain to enable leaf blade expansion.

In contrast to all above reports, Bhatia and Heisler very recently claimed that the *35S*-driven mDII-Venus control sensor also exhibits an adaxial-enrichment, which is similar to the *35S*-driven DII-Venus sensor, in the first two leaves of 3-4 DAS seedlings (Bhatia and Heisler, 2018). They further questioned if auxin is asymmetrically

distributed during early leaf development. Although activation of auxin signaling in the middle domain, which is the final output of auxin, ARF activators and repressors, remains supported by the imaging results of Bhatia and Heisler, the uneven distribution of fluorescent protein signals in the *p35S*::*mDII-VENUS* plants were clearly against previous observations.

To resolve the discrepancy, we analyzed the first two leaves of 3-4 DAS seedlings, as Bhatia and Heisler did. Consistent with all previous reports in early leaf primordia (Vernoux et al., 2011; Brunoud et al., 2012; Wang et al., 2014), but different from Bhatia and Heisler, mDII-Venus showed clear uniform distribution throughout leaf primordia qualitatively and quantitatively (Figure 1A). Although there may be variations among plants and leaves, there is no consensus uneven distribution for mDII-Venus within adaxial or abaxial domains. The DII-Venus sensor was reproducibly adxial enriched (Figure 1B), as shown before (Vernoux et al., 2011; Brunoud et al., 2012; Qi et al., 2014; Bhatia and Heisler, 2018). Bhatia and Heisler also used the R2D2 sensor to assess auxin signaling distribution in leaf primordia. We actually found slightly adaxial-enriched signals of the *pRPS5A*::*mDII-tdTomato* of R2D2 (Figure 2A). The signal of *pRPS5A*::*DII-Venus* of R2D2 was more strongly adaxial enriched (Figure 2B). Taken together, both *35S*- and *RPS5A*-driven DII/mDII sensors indicate adaxial-enriched DII signals in 3-4 DAS seedlings, which is consistent with results obtained from leaf primordia of older plants.

Given the very different expression patterns of *p35S*::*mDII-Venus* obtained by Bhatia and Heisler from all others (Vernoux et al., 2011; Brunoud et al., 2012; Wang et al., 2014), it is suggested to consider possibilities, such as seed contamination. On the other hand, the *RPS5A* promoter is active and more uniform in embryos but not in mature tissues (Weijers et al., 2001), whereas the *35S* promoter is less active in selected tissues, such as embryos. Thus, the two available DII sensors may be more suitable to different samples. The maturation time of the fluorescent protein fused to DII appears to be a key factor to the fluorescence signal (Brunoud et al., 2012). In addition, auxin-independent protein stability is clearly affecting fluorescence signal.

Thus, the use of different proteins to label DII and mDII may introduce additional variations that require further normalization.

Lastly, it is conceptually unlikely that prepatterned leaf polarity genes would lead to a uniform auxin signaling distribution as Bhatia and Heisler suggested. The proposed prepatterns of polarity genes (Husbands et al., 2009) have recently been shown experimentally (Caggiano et al., 2017; Yu et al., 2017). The adaxial-abaxial auxin difference appears after leaves bulged up (Qi et al., 2014). In fact, the prepatterned gene expression may explain different PIN distributions around the adaxial and abaxial domains (Qi et al., 2014; Shi et al., 2017). Auxin signaling is essential to translating the adaxial-abaxial prepattern into medial-lateral patterning by activating the leaf marginal domains (Guan et al., 2017). The recent proposal that wounds influence leaf adaxial-abaxial polarity (Caggiano et al., 2017) clearly ignored the extensive control experiments described by Ian Sussex and more recent researchers (Sussex, 1952; Reinhardt et al., 2005; Kuhlemeier and Timmermans, 2016).

Methods

Plant material and growth conditions.

The transgenic lines *p35S*::*DII-Venus* and *p35S*::*mDII-Venus* were obtained from Dr. Teva Vernoux, and the R2D2 reporter line was obtained from Dr. Dolf Weijers. Seeds were kept for 2 days on MS medium containing 1% sucrose in the dark at 4°C and then in the greenhouse under short-day-conditions for 3 or 4 days before imaging.

Confocal imaging and data analysis

For live imaging, seedlings grown under short-day-conditions for 3 or 4 days were transferred to the dissecting medium (3% agarose). Cotyledons were carefully removed under stereomicroscope (Nikon, SMZ18). All live imaging was performed

using 60× water dipping lens. Confocal images were taken with a Nikon A1 confocal microscope. Excitation and detection windows setups for Venus and tdTomato were as described (Qi et al., 2014). To image Venus, a 514 nm laser excitation and a 524-550 nm band-pass filter emission was used. To image tdTomato, a 561 nm laser was used for excitation and a 570-620 nm band-pass filter was used for detection.

Acknowledgements

We thank Dr. Teva Vernoux for the DII and mDII lines, and Dr. Dolf Weijers for the R2D2 line. We also thank Dr. Ying Wang for critical commenting on the manuscript.

References

Bhatia, N., and Heisler, M.G. (2018). Auxin is not asymmetrically distributed in initiating Arabidopsis leaves bioRxiv**,** 10.1101/284554.

Brunoud, G., Wells, D.M., Oliva, M., Larrieu, A., Mirabet, V., Burrow, A.H., Beeckman, T., Kepinski, S., Traas, J., Bennett, M.J., and Vernoux, T. (2012). A novel sensor to map auxin response and distribution at high spatio-temporal resolution. Nature **482,** 103-106.

Caggiano, M.P., Yu, X., Bhatia, N., Larsson, A., Ram, H., Ohno, C.K., Sappl, P., Meyerowitz, E.M., Jonsson, H., and Heisler, M.G. (2017). Cell type boundaries organize plant development. eLife **6,** e27421.

Guan, C., Wu, B., Yu, T., Wang, Q., Krogan, N.T., Liu, X., and Jiao, Y. (2017). Spatial auxin signaling controls leaf flattening in *Arabidopsis*. Curr Biol **27,** 2940-2950.

Husbands, A.Y., Chitwood, D.H., Plavskin, Y., and Timmermans, M.C. (2009). Signals and prepatterns: new insights into organ polarity in plants. Genes Dev **23,** 1986-1997.

Kuhlemeier, C., and Timmermans, M.C.P. (2016). The Sussex signal: insights into leaf dorsiventrality. Development **143,** 3230-3237.

Liao, C.Y., Smet, W., Brunoud, G., Yoshida, S., Vernoux, T., and Weijers, D. (2015). Reporters for sensitive and quantitative measurement of auxin response. Nat Methods **12,** 207-210.

Qi, J., Wang, Y., Yu, T., Cunha, A., Wu, B., Vernoux, T., Meyerowitz, E., and Jiao, Y. (2014). Auxin depletion from leaf primordia contributes to organ patterning. Proc Natl Acad Sci U S A **111,** 18769-18774.

Reinhardt, D., Frenz, M., Mandel, T., and Kuhlemeier, C. (2005). Microsurgical and laser ablation analysis of leaf positioning and dorsoventral patterning in tomato. Development **132,** 15-26.

Shi, J., Dong, J., Xue, J., Wang, H., Yang, Z., Jiao, Y., Xu, L., and Huang, H. (2017). Model

for the role of auxin polar transport in patterning of the leaf adaxial-abaxial axis. Plant J **92,** 469-480.

Sussex, I.M. (1952). Experimental and analytical studies of morphogenesis in the shoot apex of potato *Solanum tuberosum* L. (University of Manchester).

Vernoux, T., Brunoud, G., Farcot, E., Morin, V., Van den Daele, H., Legrand, J., Oliva, M., Das, P., Larrieu, A., Wells, D., Guedon, Y., Armitage, L., Picard, F., Guyomarc'h, S., Cellier, C., Parry, G., Koumproglou, R., Doonan, J.H., Estelle, M., Godin, C., Kepinski, S., Bennett, M., De Veylder, L., and Traas, J. (2011). The auxin signalling network translates dynamic input into robust patterning at the shoot apex. Mol Syst Biol **7,** 508.

Wang, Y., Wang, J., Shi, B., Yu, T., Qi, J., Meyerowitz, E.M., and Jiao, Y. (2014). The stem cell niche in leaf axils is established by auxin and cytokinin in *Arabidopsis*. Plant Cell **26,** 2055-2067.

Weijers, D., Franke-van Dijk, M., Vencken, R.J., Quint, A., Hooykaas, P., and Offringa, R. (2001). An *Arabidopsis Minute*-like phenotype caused by a semi-dominant mutation in a *RIBOSOMAL PROTEIN S5* gene. Development **128,** 4289-4299.

Yu, T., Guan, C., Wang, J., Sajjad, M., Ma, L., and Jiao, Y. (2017). Dynamic patterns of gene expression during leaf initiation. J Genet Genomics **44,** 599-601.

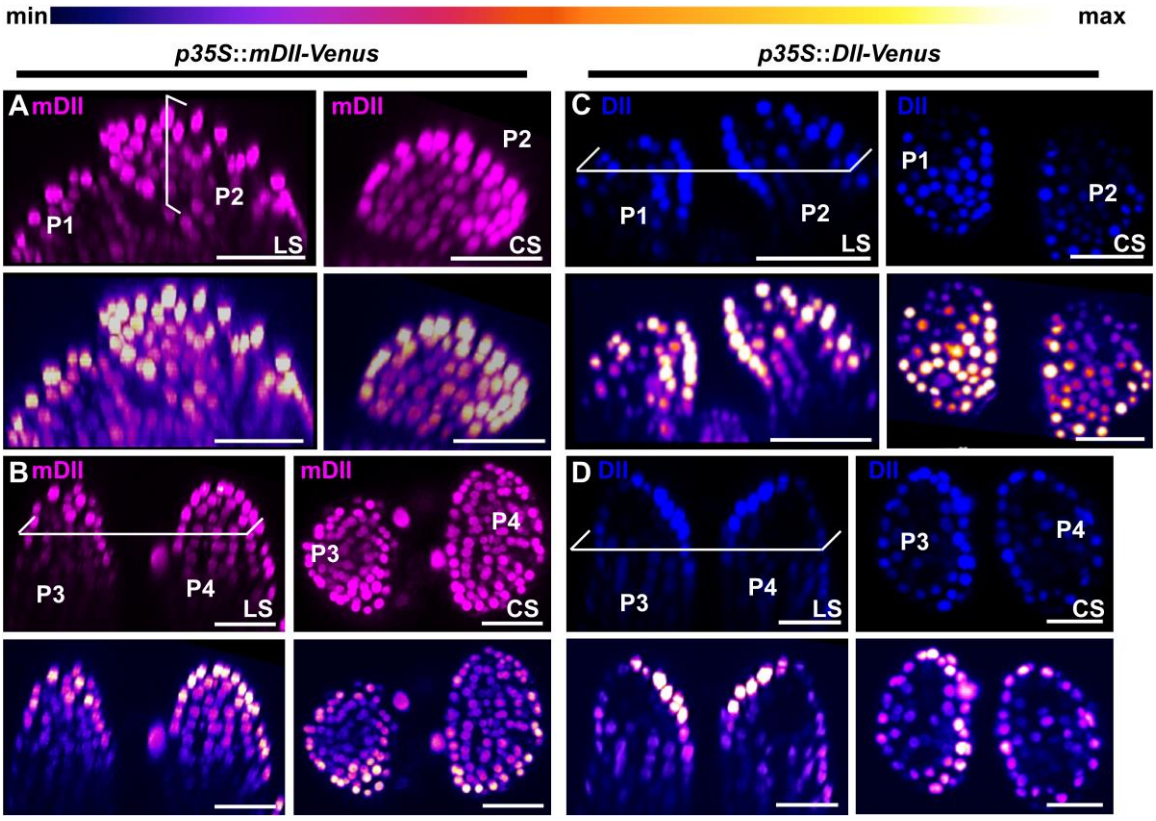

Figure 1. mDII and DII signals in young Arabidopsis leaves.

Optical sections through P1, P2, P3 and P4 leaf primordia showing expression of (**A** and **B**) mDII-Venus (magenta) and (**C** and **D**) DII-Venus (blue). LS, longitudinal section; CS, cross section. The cross section position was indicated in white lines in each longitudinal section panel. The fluorescence intensity heatmap of each panel was shown below. Scale bars, 20 μm.

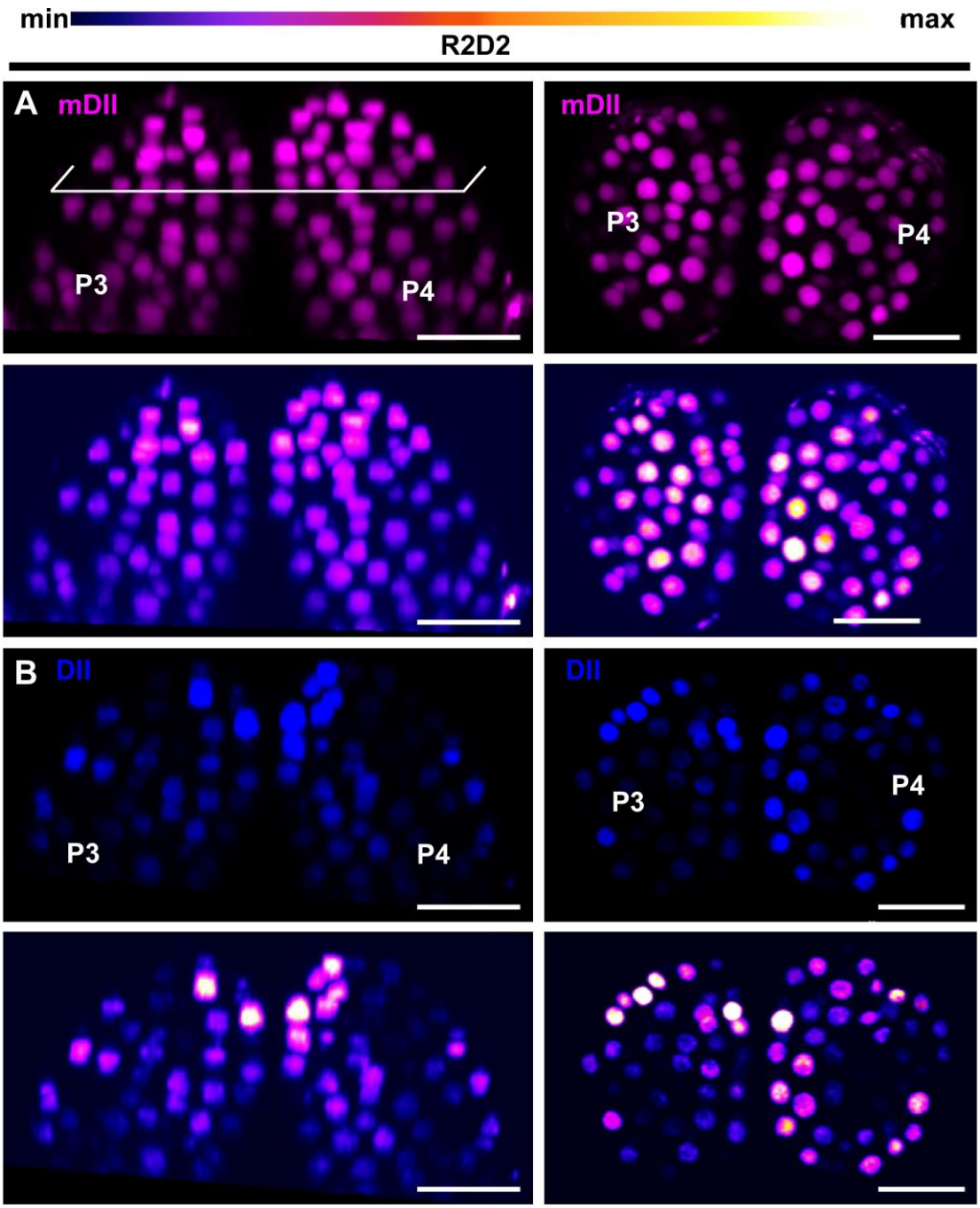

Figure 2. Predicted auxin distribution in young leaf primordia indicated by R2D2 auxin sensor.

A and **B**, Optical sections to show mDII-Venus (**A**, magenta) and DII-Venus (**B**,blue) signals in the same P3 and P4 leaf primordia, respectively. LS, longitudinal section; CS, cross section. The position of cross section was indicated in white lines in (A). The fluorescence intensity heatmap of each panel was shown below. Scale bars, 20 μm.